

ANISOTROPY OF THE MAGNETIC SUSCEPTIBILITY OF RUBY AT HELIUM TEMPERATURES

B. K. SEVAST'YANOV and V. I. BAĬBAKOV

Crystallography Institute, Academy of Sciences, U.S.S.R.; Moscow State University

Submitted to JETP editor February 11, 1964

J. Exptl. Theoret. Phys. (U.S.S.R.) **47**, 73-79 (July, 1964)

The magnetic susceptibility anisotropy of single-crystal synthetic ruby, containing between 0.016 and 1.1 wt. % Cr^{3+} , was measured at helium temperatures. The concentration of Cr^{3+} ions, isomorphously substituted into the corundum lattice, was determined from the temperature dependence of the magnetic susceptibility anisotropy.

1. INTRODUCTION

THE magnetic properties of ruby in high-frequency fields have been studied in sufficient detail, and its spectroscopic properties have also been determined (cf., for example, [1]). Brugger et al. [2,3] also investigated the magnetic susceptibility of single-crystal synthetic ruby in static magnetic fields at helium temperatures. They established a linear dependence of the Curie constant on the chromium concentration in the range from 0.047 to 1.40 wt. %. The g -factors of ruby ($g_{\parallel} = 1.82$; $g_{\perp} = 1.83$) calculated from these measurements differed from the values found by the e.s.r. method ($g_{\parallel} = 1.9840 \pm 0.0006$; $g_{\perp} = 1.9867 \pm 0.0006$). [1] This difference was ascribed to the inaccuracy in the determination of the chromium in the test samples.

Although Brugger et al. [2,3] noted that at very low temperatures ($\approx 1^{\circ}\text{K}$) the Curie constant is different along the trigonal axis of the crystal and at right angles to it, they did not carry out a detailed investigation of the magnetic susceptibility anisotropy.

As is known, [4,5] the magnetic susceptibility of ruby in the trigonal axis direction (χ_{\parallel}) and in a plane perpendicular to this axis (χ_{\perp}), is given by the expressions

$$\chi_{\parallel} = N \left\{ \alpha_{\parallel} + \frac{S(S+1)}{3kT} g_{\parallel}^2 \mu^2 - \frac{pD}{k^2 T^2} g_{\parallel}^2 \mu + \dots \right\}, \quad (1)$$

$$\chi_{\perp} = N \left\{ \alpha_{\perp} + \frac{S(S+1)}{3kT} g_{\perp}^2 \mu^2 + \frac{1}{2} \frac{pD}{k^2 T^2} g_{\perp}^2 \mu^2 + \dots \right\}. \quad (2)$$

Here, N is the number of Cr^{3+} ions which replace isomorphously the aluminum in the Al_2O_3 lattice; $S = 3/2$; $\mu = 0.9273 \times 10^{-20}$ erg/G is the Bohr magneton; $k = 1.38 \times 10^{-16}$ erg/deg is Boltzmann's constant; α_{\parallel} and α_{\perp} are the polarizabilities of ions in a magnetic field;

$$p = 1/45 S(S+1)(2S+3)(2S-1) \approx 1.$$

The most precise values of g_{\parallel} or g_{\perp} and of the initial splitting of the spin multiplet D are obviously the values of g_{\parallel} or g_{\perp} quoted above [1] and $2D = -0.3831 \pm 0.0002 \text{ cm}^{-1}$. The magnetic susceptibility anisotropy may be represented by the quantity $\Delta\chi = \chi_{\parallel} - \chi_{\perp}$ or, using Eqs. (1) and (2),

$$\Delta\chi = N \left\{ (\alpha_{\parallel} - \alpha_{\perp}) + \frac{S(S+1)}{3kT} \mu^2 (g_{\parallel}^2 - g_{\perp}^2) - \frac{pD}{k^2 T^2} \left(g_{\parallel}^2 + \frac{1}{2} g_{\perp}^2 \right) \mu^2 \right\}. \quad (3)$$

The first term ($\alpha_{\parallel} - \alpha_{\perp}$) is small compared with the second or third terms. [4] The ratio of the second to third terms in Eq. (3) amounts to $\approx 10^{-3}$ T. Therefore, at helium temperatures ($1.5-4.2^{\circ}\text{K}$), $\Delta\chi$ is governed only by the term proportional to T^{-2} , within the usual limits of the experimental error ($\approx 1-2\%$). The terms of the expansion containing higher powers of temperature will be seen to make an unimportant contribution to the value of $\Delta\chi$ and they are not included in Eq. (3).

The magnetic susceptibility anisotropy may be found conveniently from the torque acting on a sample in a uniform magnetic field. If the crystal axis makes an angle φ with the field H , the torque can be written in the form (cf., for example, [6])

$$K = 1/2 (\chi_{\parallel} - \chi_{\perp}) H^2 \sin 2\varphi, \quad (4)$$

and hence, using Eq. (3), we find that the anisotropy factor is

$$\Delta\chi = -N \frac{pD}{k^2 T^2} \left(g_{\parallel}^2 + \frac{1}{2} g_{\perp}^2 \right) \mu^2 = \frac{2K}{H^2 \sin 2\varphi}. \quad (5)$$

From the relationships (4) and (5), it follows that in polar coordinates the dependence of the torque on the angle φ should be a four-petalled rosette

with a fourfold axis of symmetry. The quantity $K/H^2 \sin 2\varphi$ should be a linear function of the quantity T^{-2} .

Since the quantities p , D , g_{\parallel} , g_{\perp} for ruby are known very accurately from spectroscopic measurements, and the torque can be measured in absolute units, Eq. (5) makes it possible to determine the absolute number N of paramagnetic Cr^{3+} ions in a ruby sample. For this purpose, it is convenient to rewrite Eq. (5) in the form

$$N = A \tan \beta, \quad (6)$$

where $A = (1.975 \pm 0.0005) \times 10^{24}$, $\tan \beta = KT^2/H^2 \times \sin 2\varphi$, and β is the angle formed by the straight line $K/H^2 \sin 2\varphi$ with the axis of $1/T^2$. We note that only trivalent chromium ions isomorphously substituted into the Al_2O_3 lattice can be detected from the susceptibility anisotropy. Nonisomorphous ions, although they give rise to a magnetic moment, make no contribution to the susceptibility anisotropy because of their disordered distribution in a crystal.

In the present work, we measured the torque acting on samples of single-crystal ruby in a uniform magnetic field at helium temperatures, using a wide range of chromium concentrations. From these measurements, we calculated the absolute number of isomorphous trivalent chromium ions in the samples.

2. EXPERIMENTAL METHOD AND SAMPLES

The torque K was measured using an improved, compared with [7], torsional magnetic balance. The details of the balance are shown in Fig. 1. A suspended system, incorporating a quartz filament 9 of ≈ 0.5 mm diameter and 63–64 cm long, is hung from a phosphor bronze filament 5 in a glass tube 14. The following items are attached to the filament 9: an arrester 7, a hollow aluminum cylinder 8, a mirror 10, an aluminum damping cylinder 11, an aluminum ring 13, and a sample 15. The damping magnetic field of ≈ 300 Oe is provided by a permanent magnet 12. The suspended system is arrested by means of sylphon bellows 2. Coils L_1 – L_4 together with the ring 13 form an induction system with negative feedback. Light from a source 22, modulated at 6 kc, is reflected by the mirror 10 and reaches two closely spaced STSV-3 photocells, which are separated by an opaque partition. The photocells are connected to the circuit of a two-channel photoamplifier which converts the modulated light beam into an alternating current fed to the coils L_1 – L_4 . When a torque acts on the suspended system, the illumination of the photo-

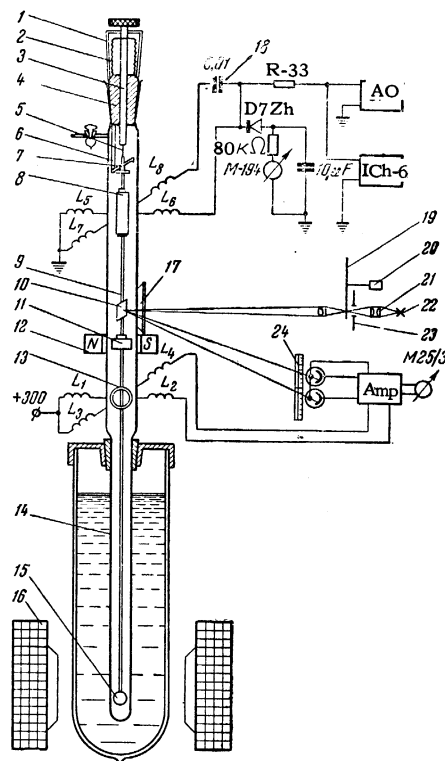


FIG. 1. Block diagram of the magnetic balance: 1) sylphon bellows frame; 2) sylphon bellows; 3) arrester rod; 4) brass joint; 5) phosphor bronze filament; 6) arrester stops; 7) arrester; 8) aluminum cylinder; 9) quartz rod of ≈ 0.5 mm diameter; 10) mirror; 11) damping cylinder; 12) permanent magnet; 13) aluminum ring; 14) glass tube; 15) sample; 16) electromagnet; 17) optical window; 18) phase-shifting capacitor; 19) modulator disk; 20) modulator motor (DAP-1); 21) and 22) light source; 23) diaphragm; 24) photocell scale.

cells changes and the alternating current in the coils L_1 – L_4 changes in such a way as to compensate the torsion. Comparisons of the current in these coils are carried out by means of a potentiometer KL-48 and a galvanometer M25/3.

It should be noted that the sensitivity of the photo-compensation system depended strongly on the mutual orientations of the plane of the ring 13 and of the axes of the coils L_1 – L_4 . Since the apparatus is reset and its position changed after every experiment, it was in practice impossible to make the sensitivity of the photo-compensation system the same in different experiments. Therefore, it was necessary to use a calibration torque for absolute measurements. For this torque, we used the interaction of the cylinder 8 with the rotating field provided by coils L_5 – L_8 . The pair of forces acting on the suspended system was determined from the current in these coils. The coils were fed from an audiofrequency oscillator (AO) working at 2300 cps, this frequency being determined by the resonance properties of the oscil-

lator and a phase-shifting capacitor 18. The generator frequency stability was checked continuously by a ICh-6 frequency meter. The current in the coils L_5 – L_8 was measured with a M-194 microammeter of class 0.5.

To obtain absolute values of K , the readings of the M-194 were calibrated using the value of the elastic constant γ of the suspension with the feedback switched off. The value of γ was found from the period of oscillations of a cylinder of known moment of inertia. The instrument was calibrated many times, using suspensions of different elastic constants ranging from ≈ 0.1 to ≈ 60 dyn-cm/deg; the instrument was thoroughly checked and the position of the cylinder 8 was varied within certain limits with respect to the coils L_5 – L_8 , etc. However, the maximum scatter of the values of the torque at a given current did not exceed $\pm 4\%$; the rms error in the value of K was not greater than $\pm 2.5\%$.

The system with the rotating field was used not only for calibration but also for compensation. The photo-compensation system served as a null indicator with a $\approx 10^{-4}$ dyn-cm sensitivity and small time constant.¹⁾

A magnetic field of up to 6 kOe intensity, was applied to a sample by a small electromagnet which could be rotated about the axis of the suspended system. The magnetic field was measured with a M-119, milliwebermeter the readings of which were first checked ballistically. The error in the field determination did not exceed $\pm 1\%$. The magnetic field uniformity was such that at distances of the order of 3–4 linear dimensions of the sample the field intensity was still the same (within the stated error).

The samples²⁾ were in the form of plane rectangular slabs 0.5 mm thick and 0.5–3 cm² in area. It is worth noting that the sample shape was unimportant in the present measurements.^[6,8]

At helium temperatures, the paramagnetic susceptibility of the sample, even at the maximum measured chromium concentration, was of the order of 10^{-4} , and the demagnetizing factor n for the ratio of the linear dimensions $\approx 1:20$ was about 0.9. It is evident from the relationship $\chi = \chi_0 / (1 + 4\pi n \chi_0)$, where χ_0 is the susceptibility of a spherical sample along a given direction, that

$$\Delta\chi = \chi_{\parallel} - \chi_{\perp} \approx (\chi_{\parallel 0} - \chi_{\perp 0}) [1 - 4\pi n(\chi_{\parallel 0} + \chi_{\perp 0})],$$

i.e., the form factor introduces a correction $\approx 10^{-4}$, which is outside the limits of the experimental error. The fact that the sample form factor was unimportant was confirmed by the symmetrical nature of the dependence $K(\varphi)$ (Fig. 2).

The slabs were cut so that their plane was perpendicular to the trigonal axis of the crystal to within 5 – 6° . In our calculations, this departure from the perpendicular orientation was neglected. It made a contribution of less than $\pm 0.5\%$ to the error in N . The weight of the samples varied from 70 mg to 6 g (cf. the table). The Cr^{3+} content, determined optically,^[9,10] amounted to 0.016–1.1 wt. %.

Usually, the measurements of $\Delta\chi(T)$ for samples with a low value of N were carried out at the maximum of the $K(\varphi)$ rosette (Fig. 2). However, in some cases, when the pair of forces acting on the sample was far too large, the angle was selected so that the photo-compensation system was not overloaded at the moment of temperature change. Thus, curve 5 in Fig. 3 was obtained for $\varphi = 15^\circ$ ($\sin 2\varphi = 0.5$). Samples Nos. 15 and 16 were measured at $\varphi = 5^\circ$. Naturally, the experimental error was greater in these cases.

3. DISCUSSION OF THE RESULTS

A typical dependence of the torque K on the angle φ at helium temperatures is shown in Fig. 2 for a fixed value of the magnetic field. In agreement with Eq. (5), the rosette in Fig. 2 has a four-fold axis.

The dependence of the quantity $K/H^2 \sin 2\varphi$, proportional to $\Delta\chi$, on $1/T^2$ is given in Fig. 3 for samples containing various amounts of chromium. The anisotropy factor rises linearly on in-

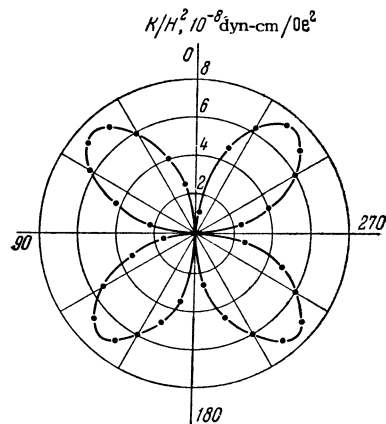


FIG. 2. Angular dependence of the quantity K/H^2 for sample No. 8 at $T = 4.2^\circ\text{K}$, $H = 2580$ Oe.

¹⁾If quartz filaments of 10 – 20μ are used as suspensions, the sensitivity of the photo-compensation system may be increased to several units per 10^{-5} dyn. cm.

²⁾We take this opportunity to thank L. M. Kharitonova, who kindly supplied the samples and analyzed them optically and M. M. Gritsenko, who carried out the chemical analysis.

Sample No.	P, mg	$\tan \beta \times 10^6$	$N \cdot 10^{-19}$	$C_m, \%$	$C_{opt}, \%$	$C_{ch}, \%$
1	239	0.18 ± 0.004	0.035	0.014 ± 0.0007	0.016	
2	330	0.32 ± 0.007	0.063	0.017 ± 0.001	0.02	0.22
3	300	0.52 ± 0.01	0.10	0.030 ± 0.0015	0.034	
4	310	1.50 ± 0.015	0.29	0.085 ± 0.0043	0.10	
5	434	11.7 ± 0.2	2.31	0.43 ± 0.022	0.51	
6	79	0.42 ± 0.009	0.083	0.88 ± 0.02	1.1	
7	671	0.97 ± 0.02	0.19	0.025 ± 0.0013		0.37
8	1090	1.27 ± 0.04	0.25	0.020 ± 0.001		0.030
9	524	2.1 ± 0.04	0.41	0.070 ± 0.0035	0.082	
10	404	0.28 ± 0.006	0.05	0.016 ± 0.0008	0.016	
11	930	1.60 ± 0.04	0.32	0.030 ± 0.0015	0.040	
12	780	1.25 ± 0.03	0.25	0.028 ± 0.0014	0.042	
13	692	1.20 ± 0.02	0.24	0.031 ± 0.0015	0.042	
14	415	0.76 ± 0.02	0.15	0.034 ± 0.002	0.041	
15	6100	84 ± 14	16.6	0.30 ± 0.06	0.5	0.57 (0.93*)
16	5900	56 ± 5	11.06	0.12 ± 0.01	0.1	0.11 (0.17*)

*Chemical analysis was carried out by two methods. For samples Nos. 15 and 16, the difference between these two methods was considerable. The table lists the values obtained by both methods.

crease of $1/T^2$. This again is in agreement with Eq. (5).

The fact that the straight lines in Fig. 3 do not pass through the origin of coordinates is a consequence of the combined effect of the diamagnetism of the lattice and of the microscopic ferromagnetic impurities which are practically always present in the sample and in the quartz filament to which it is attached. The effect of these factors is manifest also in the fact that at nitrogen temperatures, where the paramagnetic susceptibility drops by two orders of magnitude compared with its value at helium temperatures, the fourfold symmetry of the dependence $K(\varphi)$ is disturbed.

Since we measured the temperature dependence of $\Delta\chi$, the elimination of these factors was a relatively simple matter. The anisotropy of the diamagnetism of the corundum lattice at helium temperatures was approximately two orders of magnitude smaller than the anisotropy of the paramagnetic susceptibility of Cr^{3+} ions even at the lowest measured concentration of these ions (0.014%). Moreover, the diamagnetic anisotropy was independent of temperature.

As far as the ferromagnetic impurities are concerned, it is known^[11,12] that at low temperatures in fields producing saturation the susceptibility of a ferromagnet is independent of temperature to within $\approx 10^{-3}$. In the measurements described here, the saturation of the ferromagnetic impurities was reached in fields less than 1 kOe. This is illustrated, for example, by curve 4 in Fig. 3. This figure shows that the points lie practically on the same straight line.

The measurements of $\Delta\chi(T)$ were carried out in fields of 2.5–3.5 kOe, i.e., in the saturation region. The linear nature of $\Delta\chi(1/T^2)$ confirms that the influence of the ferromagnetic impurities on

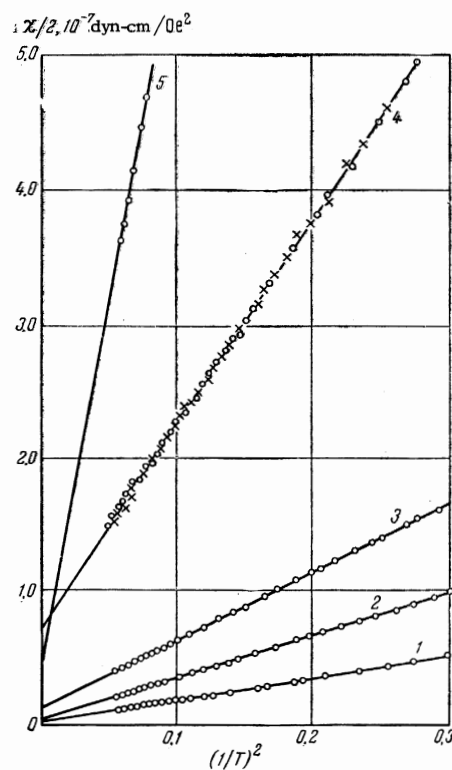


FIG. 3. Dependence of the anisotropy factor $\Delta\chi$ on $(1/T)^2$. Curve 5 was recorded using $\varphi = 15^\circ$ for sample No. 5; curve 4 was obtained for sample No. 4 using two values of the field: + 5 kOe; o 2.6 kOe; curves 1–3 were obtained for samples Nos. 1–3, respectively.

the susceptibility anisotropy is small.

The results obtained allowed us to determine the absolute number of Cr^{3+} ions in the samples. This number, N , was found using Eq. (6). The absolute sensitivity of the method in the determination of N , for a magnetic balance sensitivity of $\approx 10^{-4}$ dyn.cm in a magnetic field of 3 kOe, amounted to $\approx 10^{14}$ Cr^{3+} ions. The rms error in N for the test samples did not exceed $\pm 5\%$, except for sam-

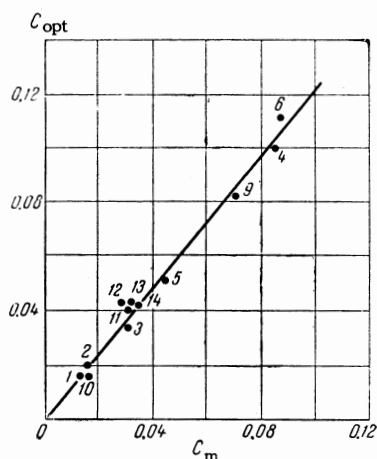


FIG. 4. Relationship between the Cr^{3+} concentration determined by optical analysis (C_{opt}) and the same concentration determined from magnetic measurements (C_m). The numbers at the points represent the sample numbers in the table.

ples Nos. 15 and 16, for which it was $\pm 15\%$ because of the lower relative accuracy in determining the angle between the field and the sample.

It seems useful to compare the values of the Cr^{3+} concentration, C , determined from chemical (C_{ch}), magnetic (C_m) and optical (C_{opt}) measurements.

The optical analysis, which is a relative method, is calibrated using the chemical analysis data for low chromium concentrations. The resultant linear relationship between the optical absorption coefficient (κ) and the Cr^{3+} concentration, C ,^[9,10] $C = 0.34 \kappa$, is then extended to higher concentrations. The values of C_{opt} and C_m are found to be proportional (Fig. 4). This also confirms that the determination of N by the magnetic method gives only the isomorphous Cr^{3+} ions because only such ions make a contribution to the optical absorption. It is evident from Fig. 4 that the straight line $C_{\text{opt}}(C_m)$ is not the bisectrix of the coordinate angle, i.e., $C_{\text{opt}} \neq C_m$. This disagreement is obviously due to the errors in calibrating the optical method using the chemical analysis measurements (points 5 and 6 are plotted on the 1:10 scale).

If we calibrate the optical analysis method using the data from the magnetic measurements, the optical coefficient is found to be related to the Cr^{3+} concentration by $C = 0.29 \kappa$. Comparison of the

chemical analysis data with the magnetic measurements shows that C_{ch} is systematically larger than C_m . This is a consequence of the fact that in chemical analysis not only the isomorphous ions but all chromium present in the sample are determined.

In conclusion, the authors thank Dr. N. A. Brilliantov for his suggestion to investigate the magnetic properties of ruby; Prof. A. I. Shal'nikov for the facilities provided in the Cryogenic Block of the Moscow State University; Prof. N. E. Alekseevskii who read the manuscript and made various valuable comments; and G. I. Kosourov and G. M. Zverev for discussing the work.

¹E. O. Schulz-Buboiss, Bell System Tech. J. 38, 271 (1959); Russ. transl. in Sbornik: Kvantovye paramagnitnye usiliteli (Collection: Quantum Paramagnetic Amplifiers), ed. by Shteinshleiger, IIL, 1961.

²K. Brugger and J. G. Daunt, Z. physik. Chem. 16, 203 (1958).

³Brugger, Snider, and Daunt, Proc. Conf. Low Temp. Phys. and Chem., Madison, 1958, p. 547.

⁴M. H. L. Price, Nuovo cimento Suppl. 6, 817 (1957); Russ. trans. in Sbornik: Kvantovye paramagnitnye usiliteli (Collection: Quantum Paramagnetic Amplifiers), ed. by Shteinshleiger, IIL, 1961.

⁵H. L. Davis, Z. physik. Chem. 16, 213 (1958).

⁶J. F. Nye, Physical Properties of Crystals, 1957 (Russ. Transl., IIL, 1960).

⁷B. K. Sevast'yanov, PTÉ No. 5, 137 (1960).

⁸N. Majumdar, Indian J. Phys. 36, 111 (1962).

⁹S. V. Grum-Grzhimaïlo and E. I. Utkina, Trudy Instituta kristallografii AN SSSR, No. 8, 99 (1953).

¹⁰Grum-Grzhimaïlo, Grechushnikov, and Gavri-shchuk, Inf. nauchno-tekhn. byull. NIChASPROM, M., No. 3, 9 (1954).

¹¹P. W. Selwood, Magnetochemistry (Russ. Transl., IIL, 1958).

¹²S. V. Vonsovskii, Sovremennoe uchenie o magnetizme (Modern Theory of Magnetism), Gostekhizdat, 1953.

Translated by A. Tybulewicz